Polish Journal of Microbiology
2019, Vol. 68, No 1, 35–42
https://doi.org/10.21307/pjm-2019-004

ORIGINAL PAPER

Mycosynthesis of Size-Controlled Silver Nanoparticles through Optimization of Process Variables by Response Surface Methodology

ASMA SHAHZAD[1], MEHWISH IQTEDAR[1]*, HAMID SAEED[2], SYED ZAJIF HUSSAIN[3], ASMA CHAUDHARY[4], ROHEENA ABDULLAH[1] and AFSHAN KALEEM[1]

[1] Department of Biotechnology, Lahore College for Women University, Lahore, Pakistan
[2] School of Pharmacy, University of the Punjab, Lahore, Pakistan
[3] Department of Chemistry, Lahore University of Management Sciences, School of Science & Engineering, Lahore, Pakistan
[4] Department of Zoology, Division of Science and Technology, University of Education, Lahore, Pakistan

Submitted 8 August 2018, revised 29 October 2018, accepted 29 October 2018

Abstract

The present study was carried out to reduce the size of silver nanoparticles (AgNPs) by optimizing physico-chemical conditions of the *Aspergillus fumigatus* BTCB10 growth based on central composite design (CCD) through response surface methodology (RSM). Variables such as a concentration of silver nitrate (mM), NaCl (%) and the wet weight of biomass (g) were controlled to produce spherical, monodispersed particles of 33.23 nm size, observing 78.7% reduction in size as compared to the initially obtained size that was equal to 356 nm. The obtained AgNPs exhibited negative zeta potential of –9.91 mV with a peak at 420 nm in the UV-Vis range whereas Fourier Transform Infrared (FT-IR) analysis identified O–H, C=C, C≡C, C–Br and C–Cl groups attached as capping agents. After conducting RSM experiments, a high nitrate reductase activity value of 179.15 nmol/h/ml was obtained; thus indicating a likely correlation between enzyme production and AgNPs synthesis. The F-value (significant at 3.91), non-significant lack of fit and determination coefficient ($R^2 = 0.7786$) is representative of the good relation between the predicted values of response. We conclude that CCD is an effective tool in obtaining significant results of high quality and efficiency.

Key words: *Aspergillus fumigatus* and AgNPs, Central Composite Design (CCD) for AgNPs synthesis, green synthesis of AgNPs, nitrate reductase activity for AgNPs synthesis

Introduction

Nanoparticles have gained acceptance in recent years due to their numerous applications. Metallic nanoparticles, with AgNPs in particular, become more popular due to their unique optical, electrical, and thermal properties and have been incorporated into products that range from photovoltaics to biological and chemical sensors as well as antimicrobial coatings in many textiles, keyboards, wound dressings, biomedical devices, nanoparticle-based fertilizers and insecticides (Li et al. 2010; Vijayan et al. 2016).

Numerous chemical methods have been developed in the past few years for the synthesis of nanoparticles. However, in order to enhance the yield and minimize the adverse effects of the process, environmental-friendly methods are being researched (Shanmuganathan et al. 2018). Nanoparticle synthesis is either done by physical, chemical or biological means. The biological method takes advantage of the natural ability of microbes – referred to as nano-factories to produce nanomaterials as metabolic by-products (Mitra et al. 2016). By employing green methods for the synthesis of nanoparticles, harmful chemicals like surfactant, enhancers, and other ionic and organic compounds are used in lower amounts (Saravanan et al. 2018b). It is now known that the reduction of silver ions to form AgNPs synthesized through microbes like bacteria and fungi is associated with NADH dependent reductase (enzymatic process) (Saravanan et al. 2018a). Furthermore, peptides such as phytochelatins prevent nanoparticle aggregations and thus maintain a balanced production within the microbes (Shankar et al. 2016).

Microbial synthesis of AgNPs can be either intracellular or extracellular and has been studied in a variety of bacteria and fungi (Das et al. 2017; Banerjee et al. 2018)

* Corresponding author: M. Iqtedar, Department of Biotechnology, Lahore College for Women University, Jail road, Lahore, Pakistan; **e-mail: miqtedar@gmail.com**

with focus on their antibacterial activity as well (Pugazhendhi et al. 2018). With their excessive secretion of extracellular enzymes, easy culturing and upscaling, fungi are suitable candidates for nanoparticle synthesis. *Aspergillus flavus, Aspergillus niger*, *Aspergillus clavatus,* and *Aspergillus fumigatus* are the fungi species studied for the mycosynthesis of nanoparticles (Zomorodian et al. 2016). The major hindrance in the microbial biosynthesis of metal nanoparticles at the industrial level is the polydispersity factor (Mitrano et al. 2016). Polydispersed nanoparticles are inconsistent and inefficient, as well as irregularities in shape can delay biological experiments, e.g. drug delivery. Additionally, a purification step is also required to enhance the quality of the nanoparticles to ensure its monodispersity which is time-consuming and adds up to the end cost (Robertson et al. 2016). The ability to regulate the size, distribution, and shape of AgNPs during the biosynthesis of AgNPs is a difficult process (Hamedi et al. 2017).

To optimize the process variables, numerous strategies have been employed but achieved little success in obtaining monodispersity (Singh et al. 2014). Classical approach of altering one parameter at a time to attain optimization has many drawbacks as numerous experiments have to be designed and time-consuming yet interaction between the parameters and their effects cannot be studied. RSM, on the other hand, uses the statistical method to design experiments and study interactions between selected variables to suggest the most suitable conditions for producing the desirable nanoparticles (Othman et al. 2017). Response Surface Methodology (RSM) is preferred over the traditional one-factor method in optimizing conditions as it minimizes the number of chemicals used along with less labor (Asghar et al. 2014).

Central Composite Design (CCD) provides excellent predictions within the design space and has more centre points as compared to others like Box-Behnken design (BBD). Moreover, it is particularly used for studying extreme conditions or values both high and low resulting in a better quadratic design (Othman et al. 2017). Hence, the present study entails the use of Central Composite Design (CCD) to obtain high-quality AgNPs from *A. fumigatus* BTCB10 by optimizing different growth condition variables and to assess the interactions between them.

Experimental

Materials and Methods

Isolation of strain and biomass preparation. *A. fumigatus* BTCB10 (GenBank accession no. KY486782) (Shahzad and Iqtedar 2017) was isolated from waste effluents of the textile industry and was grown on potato dextrose agar (PDA) at 30°C (Harrigan 1998). The media used for generating fungal biomass was according to (Mohamed et al. 2015). The pH of the media was maintained at 6.8, inoculated with fungal spores (10^5 spores/ml) and incubated at 25°C with shaking (120 rpm) for 72 hours before optimization. The biomass formed was filtered with Whatman filter paper (grade A) No. 1 (Ahlstrom, Spain) and thoroughly rinsed (three times) with sterilized distilled water to remove any traces of media. For the preparation of cell-free extract, the filtered biomass (10 g) was added to 100 ml of sterilized distilled water and incubated at 25°C with shaking (120 rpm) for 72 hours (Majeed et al. 2016).

Extracellular biosynthesis of silver nanoparticles. Cell-free extract (CFE) was prepared by filtering out the biomass and was then added to (1 mM) silver nitrate with 1:1 ratio. The mixture of CFE and $AgNO_3$ was incubated at 25°C with 120 rpm until the formation of AgNPs was indicated by the change in color from colorless to brown. The experiments were performed in triplicates with a control that was devoid of silver nitrate and only had CFE (Sadowski et al. 2008).

Characterization of silver nanoparticles. The AgNPs formed were characterized by the following techniques: for spectroscopic analysis (300 to 700 nm) of the colloidal silver UV-Vis spectrophotometer (ORI 4000 UV-Vis spectrophotometer, Germany) was used, for Particle size and zeta potential analysis – a Dynamic Light Scattering using Zeta sizer (Malvern Nano S, United Kingdom) was applied, the Fourier Transform infrared spectrophotometer ATR (Bruker-OPUS, USA) was used for the identification of functional groups, and the analysis of size and shape of the AgNPs was carried out by Atomic Force Microscopy AFM (Park systems, Korea) (Bordley et al. 2016).

Optimization and experimental design by response surface methodology. Response surface methodology was applied to analyze an estimated functional relationship among three factors by using Design Expert software (Ver. 10.0.3.1, Stat ease, Minneapolis, USA). All the variables were further narrowed down with the help of CCD i.e., central composite design (Dil et al. 2016). The optimized sample or "OS" had variables modified according to the experimental plan of three factors, which included substrate concentration (mM), a concentration of NaCl (%) and wet weight of biomass (g) denoted by A, B, and C, respectively (Table I).

The high and low values for CCD design were 3 and 1 mM for substrate concentration, 20 and 10% for NaCl concentration whereas 10 and 7 g for biomass (wet weight) (Table I). The size of biogenic AgNPs was the response (Y) that was also represented by the following equation:

$$Y = \beta_0 + \beta_1 X_1 + \beta_2 X_2 + \beta_3 X_3 + \beta_{11} X_{12} + \beta_{22} X_{22} + \\ + \beta_{33} X_{32} + \beta_{12} X_1 X_2 + \beta_{13} X_1 X_3 + \beta_{23} X_2 X_3 \quad (1)$$

Here, Y represents predicted responses, β_0 – the constant coefficient, β_1, β_2 and β_3 – the linear coefficients, β_{11}, β_{22} and β_{33} – the quadratic coefficients, β_{12}, β_{13} and β_{23} – the cross products coefficients and X_1, X_2 and X_3 were point variables. An experimental sample without RSM (i.e. without optimization), which will thereby be referred to as "WO", was also setup besides these 20 runs to compare the size of AgNPs without optimization and to study the effectiveness of the methodology.

Nitrate reductase assay. The nitrate reductase activity of fungus during AgNPs formation was done as previously described (Hamedi et al. 2017).

Results and Discussion

Characterization of AgNPs – Preliminarily observations. The production of AgNPs was at first distinguished by the color change from colorless to brown in all the samples, which occurs due to excitation of Surface Plasmon Resonance (SPR). Development of color in CFE in WO proved nanoparticle synthesis, which was necessary before commencing optimization of the experiment (Fig. 1A). After the completion of optimization experiments under RSM, the OS also exhibited the color change to a medium-brown, verifying the synthesis of AgNPs (Fig. 2A), similarly as it was demonstrated in the studies with *Fusarium acuminatum* (Khan et al. 2018) and *A. fumigatus* (Ghanbari et al. 2018).

Table I
Central composite design (CCD) matrix of three independent variables for AgNPs biosynthesis in codes with experimental results.

Runs	Factor A: Substrate concentration (mM)	Factor B: NaCl concentration (%)	Factor C: Wet weight of biomass (g)	Response: Size of AgNPs (nm)
1	1	10	7	33.65
2	3	20	7	127.20
3	2	15	8.5	68.23
4	1	20	10	33.65
5	3	1	10	76.22
6	1	20	7	33.65
7	2	15	8.5	68.20
8	2	15	8.5	68.30
9	2	23.41	8.5	89.37
10	1	10	10	33.65
11	3	20	10	70.48
12	3.68	15	8.5	156.2
13	2	15	11.02	33.65
14	2	15	8.5	33.55
15	2	15	8.5	33.65
16	0.32	15	8.5	126.30
17	2	15	5.98	33.23
18	2	6.59	8.5	33.45
19	3	10	7	127.10
20	2	15	8.5	90.06

Characterization of AgNPs – UV-Vis spectroscopy. The UV-Vis spectra were also analyzed, and demonstrated WO peak formation at 452 nm (λ max) (Fig. 1A) and 420 nm (λ max) for OS (Fig. 2A). The result showed a significant difference between both situations, with the latter possessing a lower wavelength, which suggests the fabrication of small-sized AgNPs (Hamedi et al. 2017). Similarly, other studies on mycosynthesis have also reported the formation of AgNPs having SPR band at 420 nm with *F. acuminatum*, *A. niger* and *A. flavus* (Khan et al. 2018).

DLS analysis – Before optimization. The WO AgNPs produced larger sized nanoparticles. Their size was analyzed by zeta sizer as shown in Fig. 1B. The observed average value was 356 nm with a polydispersion index (PDI) of 0.42. Two peaks were formed of which peak one had a value of 375.0 nm with 95.8% intensity, and peak 2 presented at 5200 nm with 4.2% intensity. The sample displayed high polydispersion without the RSM. Over 100 nm-sized nanoparticles were synthesized with *A. terreus* (Rathna et al. 2013) whereas *Pleurotus sajorcaju* formed AgNPs of 5 to 50 nm (Khan et al. 2018).

DLS analysis – After optimization. The OS AgNPs were 33.23 nm with very lower PDI i.e. 0.12 having the single peak in UV-vis spectrum (Fig. 2B). Small size and less PDI both are important properties of nanoparticles that greatly influence the activity of NPs in different applications such as antimicrobial activity, increase interaction with the targeting site (Vijayan et al. 2016). The previous study on the fungal mediated synthesis of AgNPs from *Aspergillus oryzae* reported polydisperse particles; displaying size in 6–26 nm (El-Batal et al. 2017). The zeta potential (–9.91 mV) of the OS (Fig. 2C) indicated stable AgNPs formation. Zeta potential is another important property of NPs that is required for efficient performance in different applications such as long-term usage and application in the different environment without affecting the activity (Vijayan et al. 2016). A comparison with WO particle sizes and PDIs revealed that the smaller sized AgNPs were indeed produced under RSM conditions and no such polydispersity was observed.

Atomic Force Microscopy (AFM). The WO AgNPs produced were not only larger in size but also revealed triangular-shaped nanoparticles (Fig. 1C). OS AgNPs were found to be spherical under AFM (Fig. 2D).

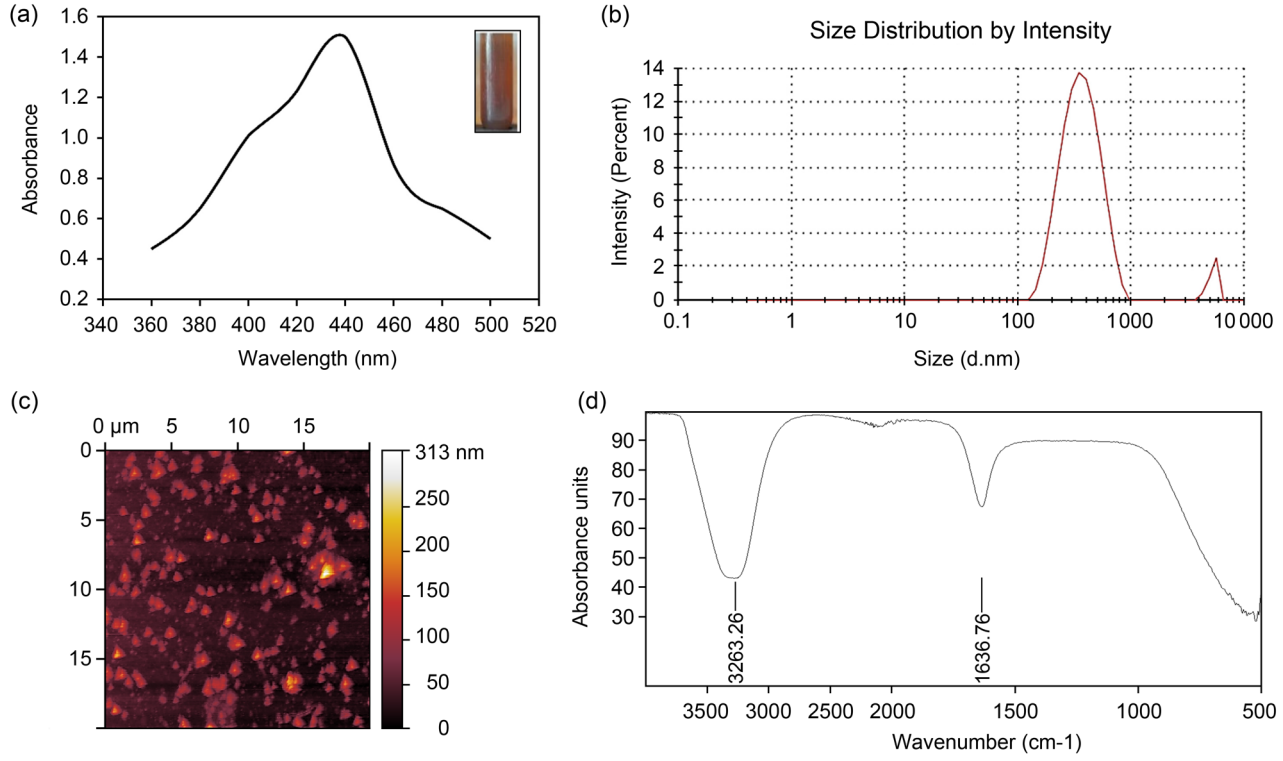

Fig. 1. Characterization of AgNPs obtained WO.

A. UV-Vis spectrophotometer analysis representing a peak of AgNPs at 452 nm and showing brown coloured nanoparticles. B. Zeta sizer (DLS) analysis representing peak at 356nm nm. C. Triangular shaped AgNPs revealed by AFM. D. Fourier transform infrared (FT-IR) analysis of AgNPs.

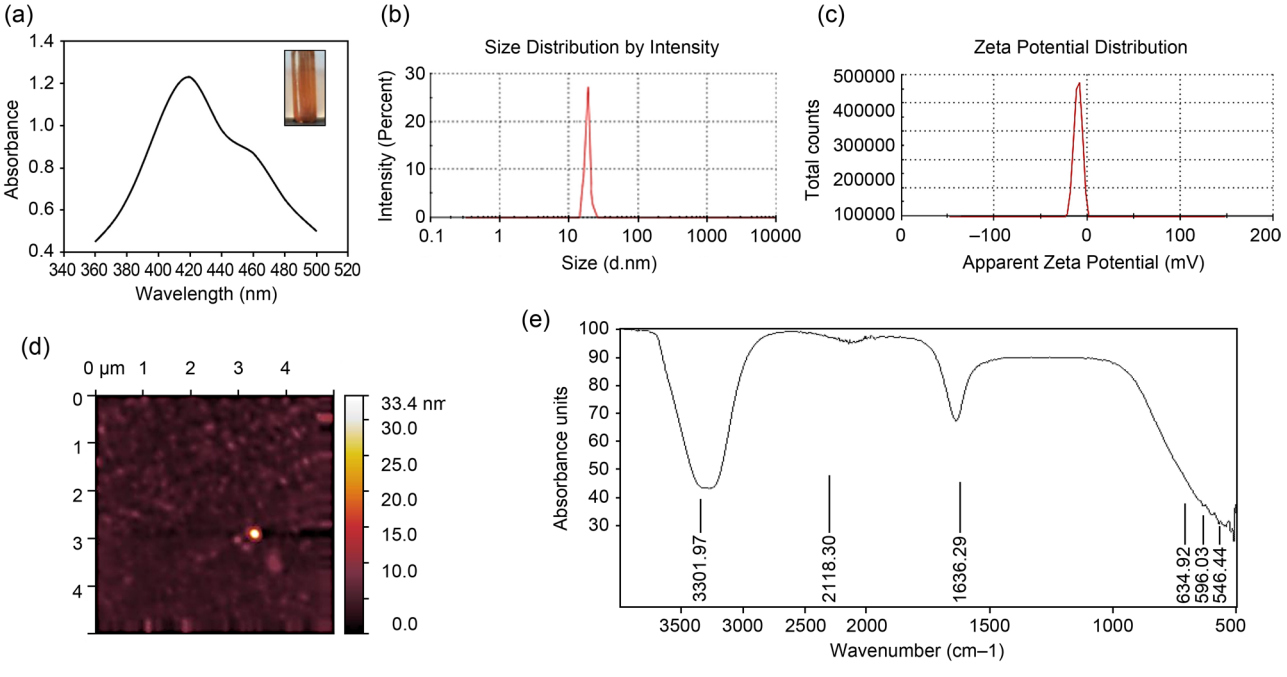

Fig. 2. Characterization of AgNPs obtained OS.

A. UV-Vis spectrophotometer analysis representing peak of AgNPs at 420 nm and showing medium brown coloured nanoparticles. B. Zeta sizer (DLS) analysis representing peak at 33.23 nm. C. Zeta potential analysis by DLS. D. Spherical shaped AgNPs revealed by AFM. E. Fourier transform infrared (FT-IR) analysis of AgNPs indicating presence of functional groups.

Othman et al. (2017) also achieved spherical shaped AgNPs using *Trichoderma viride* under RSM conditions.

FTIR spectroscopy – Before optimization. The biomolecules that are present in the cell-free extract have the capability to bind themselves with metallic nanoparticles and act as capping agents (Gudikandula et al. 2017). Functional groups identified in WO sample were N-H (3263.26 cm^{-1}) and C = C (1636.76 cm^{-1}) (Fig. 1D).

FTIR spectroscopy – After optimization. Functional groups as capping agents involved in the stability of OS AgNPs and the prevention of their aggregation were identified as O–H, C≡C and C=C by FT-IR analysis. The FTIR spectra presented an absorption band at 3301.97 cm^{-1}, which corresponded to the stretching vibrations of alcohol (Fig. 2E). While the other absorption bands were at 2118.30 cm^{-1} and 1636.29 cm^{-1}, assigned to the stretching vibrations of alkyne sand alkenes respectively. Three more bands were observed at 634.92 cm^{-1}, 596.03 cm^{-1}, and 546.44 cm^{-1}, which represented the C-Cl and C-Br groups (Fig. 2C). A similar study has also reported the presence of such groups in conferring the stability of AgNPs; C – C, – COO –, – C = C– and C–N were other functional groups found in a study with AgNPs formed by *F. oxysporum* (Hamedi et al. 2017). Type of capping agents helps not only in stabilizing the NPs but also to attach them to different ligands and drugs for site-specific targeting (Majeed et al. 2016).

Nitrate reductase assay. The presence of extracellular proteins in the medium of fungi is believed to play a significant role in the synthesis and stabilization of AgNPs. NADH has been reported to be responsible for the formation of AgNPs and reduction of silver nitrate to its colloidal state (Jogee et al. 2017) as illustrated (Fig. 3A). High enzyme activity was observed throughout the experiments, with the highest being 179.15 nmol/h/ml (Fig. 3B). All the OS experimental runs produced monodispersed AgNPs. At higher substrate and metal salt concentration, the enzyme activity seemed delayed and larger sized AgNPs were formed; which could be due to unavailability of functional groups that were responsible for carrying out reduction processes.

At comparatively lower substrate and metal concentration, the smaller-sized silver nanoparticles were produced with rapid synthesis rate possibly due to the presence of greater number of functional groups. Devi et al. (2013) has highlighted the correlation of nitrate reductase activity with nanoparticle synthesis and reported that *Trichoderma asperellum,* produced 200 (nmol/h/ml) of enzyme hence leading to the formation of stable AgNPs. According to our study sample number 13 produced 179.15 (nmol/h/ml) of enzyme leading to formation of small-sized AgNPs 33.65 nm, which could be due to secretion of the abundant enzyme.

The substrate concentration (mM) is defined by A, whereas the concentration of NaCl (%) by B and wet weight of biomass (g) is denoted by C, Y represents

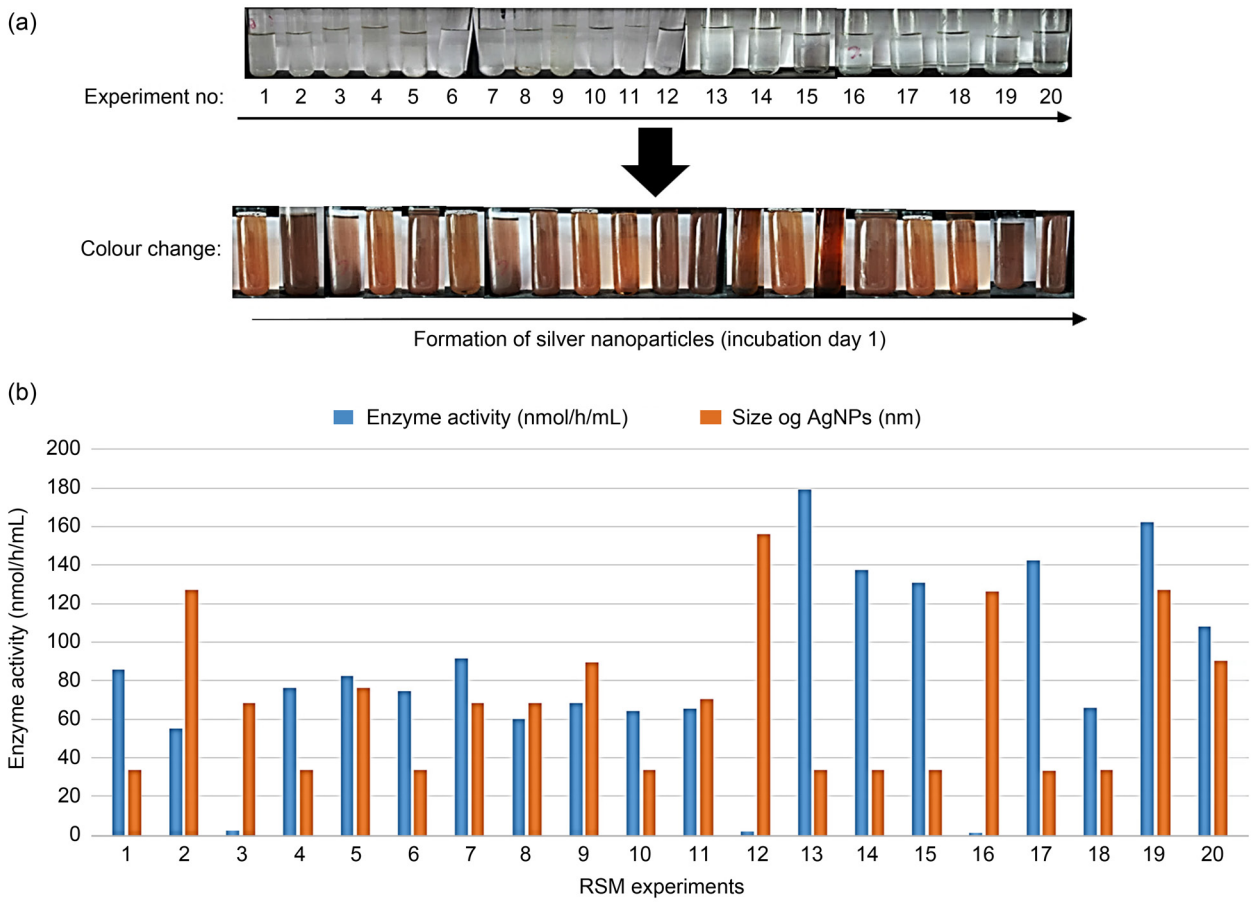

Fig. 3. A. Colour change observed during the optimization experiments (20 runs). B. Estimation of nitrate reductase activity (nmol/h/ml) and reduction in the size of AgNPs during different RSM experiments.

Table II
Analysis of Variance (ANOVA) of the Fitted Quadratic Model and regression analysis for optimization of AgNPs biosynthesis.

Source	Sum of Squares	Df	Mean Square	F-Value	*p*-value	Prob > F
Model	23241.50	9	2582.39	3.91	0.0224	Significant
A – Substrate concentration	7343.55	1	7343.55	11.11	0.0076	Significant
B – NaCl concentration	572.28	1	572.28	0.87	0.3740	
C – Wet weight of biomass	836.67	1	836.67	1.27	0.2868	
AB	3.98	1	3.98	0.006017	0.9397	
AC	1447.22	1	1447.22	2.19	0.1697	
BC	4.26	1	4.26	0.006451	0.9376	
A^2	9658.74	1	9658.74	14.62	0.0034	Significant
B^2	78.85	1	78.85	0.12	0.7369	
C^2	2154.83	1	2154.83	3.26	0.1011	
Residual	6608.52	10	660.85			
Lack of Fit	4113.14	5	822.63	1.65	0.2984	Not significant
Pure Error	2495.38	5	499.08			
Core Total	29850.02	19				
Std. dev	C.V	R-Squared	Adj R-Squared	Pred R-Squared	Adeq Precision	
25.71	37.53	0.7786	0.5794	0.1664	8.801	

the size of AgNPs. The analysis of variance (ANOVA) for the size of AgNPs is presented (Table II). Optimum response (33.23 nm AgNPs) was recorded with 2 mM silver nitrate concentration, 5.98 g biomass wet weight and 15% NaCl concentration. The results reflected that model was statistically significant with the confidence level of 95%, F-value of 3.91 and low probability P-value of < 0.0224. By comparing the viability of current model residuals to the variability between observations at replicate settings of the factors, the lack of fit test was performed.

The lack of fit test with F-value 1.65 and P-value 0.2984 was statistically non-significant. The insignificant lack of fit test indicated that there might be some systematic variations in the hypothesized model, which can be accounted because of replicate values of the independent variable and gave an estimate of the pure error in the model. In one of the studies with *Trichoderma viride,* RSM analysis showed a low value of 1.70 with lack of fit test, which also proved the significance of the model (Othman et al. 2017).

The values of determination coefficients R^2 and R^2_{adj} were calculated as 0.7786 and 0.5794, which measured the reliability of model. This indicated that approximately 77.86% was attributed to the variables and it indicated the significance of the model. Study with *T. viride* also illuminated coefficients R^2 (0.7246) and R^2_{adj} (0.8886) after conducting RSM experiments and indicated the reliability of model. The coefficient of variation (CV) is indicative of the degree of precision of all the compared treatments hence lower value of CV (37.53%) approved the certainty of the model in our study. The RSM study with *T. viride* (Othman et al. 2017) also showed a lower value CV (28.67%) proving the accuracy of the model.

Analysis of 3D surface plots. A three-dimensional response surface plot illustrated the relationship between two process variables and the third one presents its optimized condition for the variables (smallest size of AgNPs). The two-dimensional contour plot specified the interaction between the dependent and independent process variables by forming different shapes like elliptical or circular depending upon the relationship between the parameters. The plots (Fig. 4A and Fig. 4B) showed a stronger interaction between metal salt (% NaCl) and substrate (mM) concentration.

It clarifies that the size of the AgNPs had increased by increasing substrate concentration (mM) while the increase in metal salt concentration would lead to the decreased size of AgNPs. The graphs (Fig. 4C) depicted the negligible interaction between metal salt concentration and weight of biomass. The increase in salt concentration caused a slight increase in the size of particles but maximum salt concentration would have resulted in smaller AgNPs. The plots further illustrated the relationship between substrate concentration and wet biomass weight. Decreased size of AgNPs was observed at minimum substrate concentration and wet biomass weight. The results corroborated the hypothesis i.e., the decreased size of AgNPs.

Conclusively, by designing experiments using Response Surface Methodology (RSM) based on Cen-

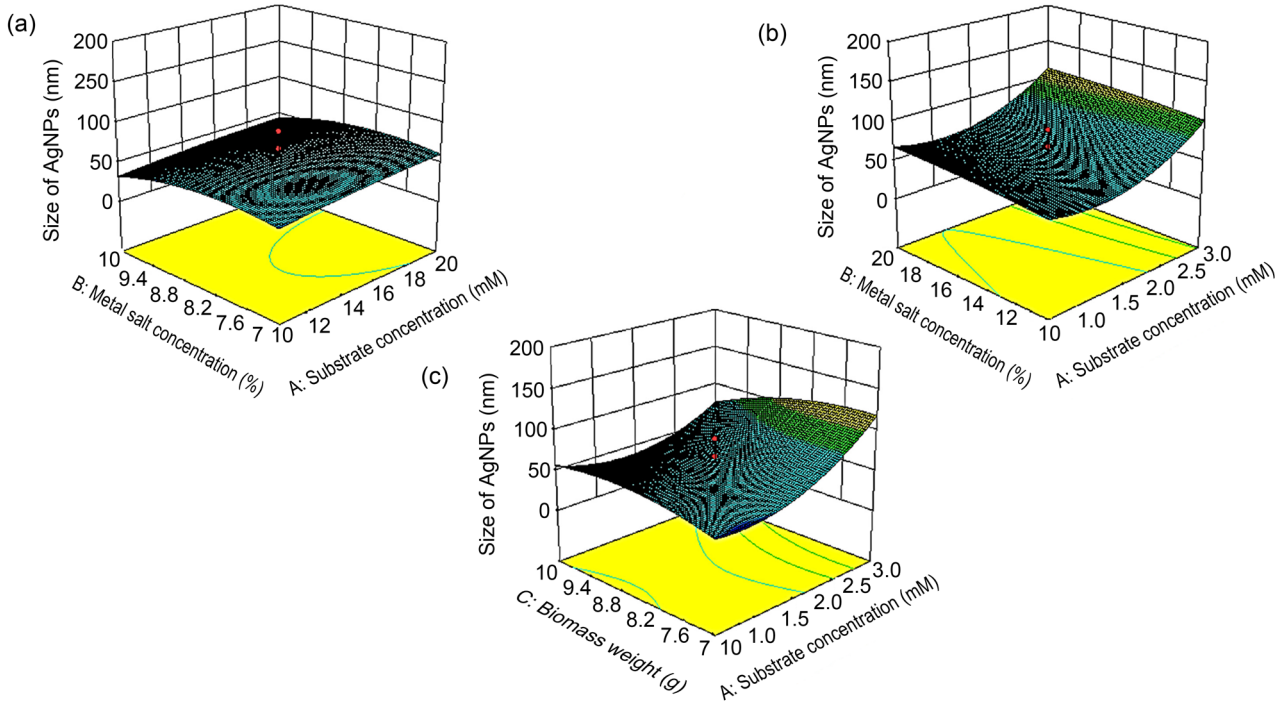

Fig. 4. 3D surface plots analysis. A. Effect of substrate concentration and metal salt concentration. B. Effect of metal salt concentration and substrate concentration. C. Effect of substrate concentration and wet weight of biomass.

tral Composite Design (CCD) about 78.7% reduction in size was observed from the sample without RSM optimization. Hence the method proved to be successful, eco-friendly and low-cost for the efficient synthesis of AgNPs with fungus *A. fumigatus* (BTCB10).

Acknowledgements

The authors greatly acknowledge the financial support provided under the Institutional Strengthening Program and Access to Scientific Instrument Program by the Higher Education Commission (HEC) Pakistan.

Conflict of interest

The authors do not report any financial or personal connections with other persons or organizations, which might negatively affect the contents of this publication and/or claim authorship rights to this publication.

Literature

Asghar A, Abdul Raman AA, Daud WMAW. A comparison of central composite design and Taguchi method for optimizing Fenton process. Sci World J. 2014;2014:1–14. doi:10.1155/2014/869120 Medline

Banerjee K, Ravishankar Rai V. A review on mycosynthesis, mechanism, and characterization of silver and gold nanoparticles. Bionanoscience. 2018;8(1):17–31. doi:10.1007/s12668-017-0437-8

Bordley JA, El-Sayed MA. Enhanced electrocatalytic activity toward the oxygen reduction reaction through alloy formation: Platinum-silver alloy nanocages. J Phys Chem C. 2016;120(27):14643–14651. doi:10.1021/acs.jpcc.6b03032

Das RK, Pachapur VL, Lonappan L, Naghdi M, Pulicharla R, Maiti S, Cledon M, Dalila LMA, Sarma SJ, Brar SK. Biological synthesis of metallic nanoparticles: plants, animals and microbial aspects. Nanotechnol Environ Eng. 2017;2(1):18. doi:10.1007/s41204-017-0029-4

Devi TP, Kulanthaivel S, Kamil D, Borah JL, Prabhakaran N, Srinivasa N. Biosynthesis of silver nanoparticles from *Trichoderma* species. Indian J Exp Biol. 2013;51(7):543–547. Medline

Dil EA, Ghaedi M, Ghaedi A, Asfaram A, Jamshidi M, Purkait MK. Application of artificial neural network and response surface methodology for the removal of crystal violet by zinc oxide nanorods loaded on activate carbon: kinetics and equilibrium study. J Taiwan Inst Chem Eng. 2016;59(59):210–220. doi:10.1016/j.jtice.2015.07.023

Ghanbari S, Vaghari H, Sayyar Z, Adibpour M, Jafarizadeh-Malmiri H. Autoclave-assisted green synthesis of silver nanoparticles using *A. fumigatus* mycelia extract and the evaluation of their physico-chemical properties and antibacterial activity. Green Processing and Synthesis. 2018;7(3):217–224. doi:10.1515/gps-2017-0062

Gudikandula K, Vadapally P, Singara Charya MA. Biogenic synthesis of silver nanoparticles from white rot fungi: their characterization and antibacterial studies. OpenNano. 2017;2(1):64–78. doi:10.1016/j.onano.2017.07.002

Hamedi S, Ghaseminezhad M, Shokrollahzadeh S, Shojaosadati SA. Controlled biosynthesis of silver nanoparticles using nitrate reductase enzyme induction of filamentous fungus and their antibacterial evaluation. Artif Cells Nanomed Biotechnol. 2017;45(8):1588–1596. doi:10.1080/21691401.2016.1267011 Medline

Hamedi S, Shojaosadati SA, Shokrollahzadeh S, Hashemi-Najaf Abadi S. Controlled biosynthesis of silver nanoparticles using culture supernatant of filamentous fungus. Iran J Chem Chem Eng. 2017;36(5):33–42.

Harrigan W. Laboratory methods in food microbiology. San Diego (USA): Academic Press. 1998;100 p.

Jogee PS, Ingle AP, Rai M. Isolation and identification of toxigenic fungi from infected peanuts and efficacy of silver nanoparticles against them. Food Control. 2017;71:143–151. doi:10.1016/j.foodcont.2016.06.036

Khan AU, Malik N, Khan M, Cho MH, Khan MM. Fungi-assisted silver nanoparticle synthesis and their applications. Bioprocess Biosyst Eng. 2018;41(1):1–20. doi:10.1007/s00449-017-1846-3 Medline

Li WR, Xie XB, Shi QS, Zeng HY, OU-Yang YS, Chen YB. Antibacterial activity and mechanism of silver nanoparticles on *Escherichia coli.* Appl Microbiol Biotechnol. 2010;85(4):1115–1122. doi:10.1007/s00253-009-2159-5 Medline

Majeed S, Abdullah MS, Dash GK, Ansari MT, Nanda A. Biochemical synthesis of silver nanoprticles using filamentous fungi *Penicillium decumbens* (MTCC-2494) and its efficacy against A-549 lung cancer cell line. Chin J Nat Med. 2016;14(8):615–620. doi:10.1016/S1875-5364(16)30072-3 Medline

Mitra C, Ghoshroy S, Lead J, Chanda A. Decreased aflatoxin biosynthesis upon uptake of 20 nm-sized citrate coated silver nanoparticles by the aflatoxin producer *Aspergillus parasiticus.* Microsc Microanal. 2016;22 S3:1182–1183. doi:10.1017/S1431927616006759

Mitrano DM, Lombi E, Dasilva YAR, Nowack B. Unraveling the complexity in the aging of nanoenhanced textiles: A comprehensive sequential study on the effects of sunlight and washing on silver nanoparticles. Environ Sci Technol. 2016;50(11):5790–5799. doi:10.1021/acs.est.6b01478 Medline

Mohamed YM, Azzam AM, Amin BH, Safwat NA. Mycosynthesis of iron nanoparticles by *Alternaria alternata* and its antibacterial activity. Afr J Biotechnol. 2015;14(14):1234–1241. doi:10.5897/AJB2014.14286

Othman AM, Elsayed MA, Elshafei AM, Hassan MM. Application of response surface methodology to optimize the extracellular fungal mediated nanosilver green synthesis. JGEB. 2017;15(2):497–504.

Pugazhendhi A, Prabakar D, Jacob JM, Karuppusamy I, Saratale RG. Synthesis and characterization of silver nanoparticles using *Gelidium amansii* and its antimicrobial property against various pathogenic bacteria. Microb Pathog. 2018;114(114):41–45. doi:10.1016/j.micpath.2017.11.013 Medline

Rathna GS, Elavarrsi A, Peninal S, Subramanian J, Mano G, Kalaiselvam M. Extracellular biosynthesis of silver nanoparticles by endophytic fungus *Aspergillus terreus* and its anti-dermatophytic activity. Int J Pharm Biol Arch. 2013;1(4):481–487.

Robertson JD, Rizzello L, Avila-Olias M, Gaitzsch J, Contini C, Magoń MS, Renshaw SA, Battaglia G. Purification of nanoparticles by size and shape. Sci Rep. 2016;6(1):27494. doi:10.1038/srep27494 Medline

Sadowski Z, Maliszewska IH, Grochowalska B, Polowczyk I, Kozlecki T. Synthesis of silver nanoparticles using microorganisms. Mater Sci Pol. 2008;26(2):419–424.

Saravanan M, Arokiyaraj S, Lakshmi T, Pugazhendhi A. Synthesis of silver nanoparticles from *Phenerochaete chrysosporium* (MTCC-787) and their antibacterial activity against human pathogenic bacteria. Microb Pathog. 2018a;117(117):68–72. doi:10.1016/j.micpath.2018.02.008 Medline

Saravanan M, Barik SK, MubarakAli D, Prakash P, Pugazhendhi A. Synthesis of silver nanoparticles from *Bacillus brevis* (NCIM 2533) and their antibacterial activity against pathogenic bacteria. Microb Pathog. 2018b;116(116):221–226. doi:10.1016/j.micpath.2018.01.038 Medline

Shahzad A, Iqtedar M. *Aspergillus fumigatus* isolate BTCC10 small subunit ribosomal RNA gene (KY486782) [Internet]. NCBI. 2017; [cited 2018 September 16]. Available from: https://www.ncbi.nlm.nih.gov/nuccore/KY486782

Shankar PD, Shobana S, Karuppusamy I, Pugazhendhi A, Ramkumar VS, Arvindnarayan S, Kumar G. A review on the biosynthesis of metallic nanoparticles (gold and silver) using bio-components of microalgae: formation mechanism and applications. Enzyme Microb Technol. 2016;95(95):28–44. doi:10.1016/j.enzmictec.2016.10.015 Medline

Shanmuganathan R, MubarakAli D, Prabakar D, Muthukumar H, Thajuddin N, Kumar SS, Pugazhendhi A. An enhancement of antimicrobial efficacy of biogenic and ceftriaxone-conjugated silver nanoparticles: green approach. Environ Sci Pollut Res Int. 2018;25(11):10362–10370. doi:10.1007/s11356-017-9367-9 Medline

Singh D, Rathod V, Ninganagouda S, Hiremath J, Singh AK, Mathew J. Optimization and characterization of silver nanoparticle by endophytic fungi *Penicillium* sp. isolated from *Curcuma longa* (turmeric) and application studies against MDR *E. coli* and *S. aureus.* Bioinorg Chem Appl. 2014;2014:1–8. doi:10.1155/2014/408021 Medline

Vijayan SR, Santhiyagu P, Ramasamy R, Arivalagan P, Kumar G, Ethiraj K, Ramaswamy BR. Seaweeds: A resource for marine bionanotechnology. Enzyme Microb Technol. 2016;95(95):45–57. doi:10.1016/j.enzmictec.2016.06.009 Medline

Zhao X, Zhou L, Riaz Rajoka MS, Yan L, Jiang C, Shao D, Zhu J, Shi J, Huang Q, Yang H, et al. Fungal silver nanoparticles: synthesis, application and challenges. Crit Rev Biotechnol. 2018;38(6):817–835. doi:10.1080/07388551.2017.1414141 Medline

Zomorodian K, Pourshahid S, Sadatsharifi A, Mehryar P, Pakshir K, Rahimi MJ, Arabi Monfared A. Biosynthesis and characterization of silver nanoparticles by *Aspergillus* species. BioMed Res Int. 2016;2016:1–6. doi:10.1155/2016/5435397 Medline